Magnetic circular dichroism studies of exogenous ligand and substrate binding to the non-heme ferrous active site in phthalate dioxygenase

Elizabeth G Pavel[1], Laura J Martins[2], Walther R Ellis, Jr[2], and Edward I Solomon[1]*

[1]Department of Chemistry, Stanford University, Stanford, CA 94305, USA and [2]Department of Chemistry, University of Utah, Salt Lake City, UT 84112, USA

Background: Mononuclear non-heme iron centers are found in the active sites of a variety of enzymes that require molecular oxygen for catalysis. The mononuclear non-heme iron is believed to be the active site for catalysis, and is presumed to bind and activate molecular oxygen. The mechanism of this reaction is not understood. Phthalate dioxygenase is one such enzyme. Because it also contains a second iron site, the Rieske site, it is difficult to obtain information on the structure of the active site. We therefore used magnetic circular dichroism (MCD) spectroscopy to probe the mononuclear non-heme Fe^{2+} site in this biodegradative enzyme.

Results: The MCD spectrum of the resting enzyme shows features indicative of one six-coordinate Fe^{2+} site; substrate binding converts the site to two different five-coordinate species, opening up a coordination position for O_2 binding. MCD spectra of the corresponding apoenzyme have been subtracted to account for temperature-independent contributions from the Rieske site. Azide binds both to the resting enzyme to produce a new six-coordinate species, showing that one of the ferrous ligands is exchangeable, and also to the enzyme-substrate complex to form a ternary species. The low azide binding constant for the substrate–enzyme species relative to the resting enzyme indicates steric interaction and close proximity between exogenous ligand and the substrate.

Conclusions: We have been able to provide some detailed structural insight into exogenous ligand and substrate binding to the non-heme Fe^{2+} site, even in the presence of the enzyme's [2Fe–2S] Rieske center. Further mechanistic studies are now required to maximize the molecular-level detail available from these spectroscopic studies.

Chemistry & Biology November 1994, 1:173–183

Key words: NIR MCD, non-heme ferrous, phthalate dioxygenase, Rieske

Introduction

Mononuclear non-heme iron centers are present at the active sites of a variety of enzymes which require dioxygen for catalysis, often involving the interaction of molecular oxygen with the iron for activation [1–3]. These enzymes include soybean lipoxygenase [4] (which catalyzes the hydroperoxidation of unsaturated lipids), the intradiol dioxygenase metapyrocatechase [5] and the extradiol dioxygenase protocatechuate 3,4-dioxygenase [6] (catechol ring cleavage), phenylalanine hydroxylase [7] (tetrahydropterin-dependent hydroxylation of aromatic rings), clavaminate synthase [8] (an α-ketoglutarate-dependent enzyme which can perform hydroxylation, β-lactam ring closure, or desaturation, depending on substrate), ω-hydroxylase [9] (hydroxylation of alkanes and fatty acids), phthalate dioxygenase [10] (*cis*-dihydroxylation of unactivated aromatics), and the anti-cancer drug bleomycin [11,12] (DNA cleavage).

Phthalate dioxygenase (PDO) is one member of a broader class of environmentally-significant bacterial dioxygenases which activate aromatic substrates for further degradation and catabolism. This family of enzymes includes benzene dioxygenase [13], benzoate dioxygenase [14], naphthalene dioxygenase [15], pyrazon dioxygenase [16], and toluene dioxygenase [17], all of which contain a [2Fe–2S] Rieske site and a mononuclear non-heme iron. In addition to the bacterial dioxygenases, there are other enzymes which also contain the Rieske cluster plus mononuclear non-heme iron motif: 4-chlorophenylacetate 3,4-dioxygenase, which converts substrate to catechol with chloride elimination [18], vanillate demethylase, which participates in the biodegradation of lignin [19], and 4-methoxybenzoate *O*-demethylase (putidamonooxin), which catalyzes the conversion of 4-methoxybenzoic acid to 4-hydroxybenzoic acid and formaldehyde [20]. In all of these systems, the mononuclear non-heme iron is believed to be the active site for catalysis and presumably binds and activates molecular oxygen. We and others have chosen to study phthalate dioxygenase as representative of these enzymes because of its availability in high yield and stability.

PDO catalyzes the *cis*-dihydroxylation of phthalate to 1,2-dihydroxy-4,5-dicarboxy-3,5-cyclohexadiene in the presence of phthalate dioxygenase reductase (PDR), NADH as an electron source and O_2. This reaction is the first of four steps in the biodegradation pathway of

*Corresponding author.

phthalate (see Fig. 1). Both phthalate dioxygenase and its reductase PDR are isolated from *Pseudomonas cepacia* grown on phthalate as the sole carbon and energy source. The reductase is a 34-kDa flavin mononucleotide/[2Fe–2S] protein for which a crystal structure has recently been reported [21]. The dioxygenase is a large enzyme composed of four identical 48-kDa subunits. Each subunit contains one [2Fe–2S] Rieske cluster and one mononuclear non-heme iron center [10]. The Rieske cluster serves as an electron storage site and is similar to the plant ferredoxin [2Fe–2S] centers in that the two irons are tetrahedrally coordinated and are bridged by two sulfides; however, while each of the irons in a ferredoxin site is ligated to two Cys sulfurs, one iron of the Rieske site is ligated to two Cys sulfurs and the other to two His nitrogens. Correspondingly, the redox potentials of Rieske proteins are generally higher than those of the ferredoxins (+350mV to −150 mV versus approximately −400 mV) [22].

The mononuclear non-heme iron is required for maximal activity, though other metals (Ni^{2+}, Co^{2+}, Mn^{2+}, Cu^{2+}, Zn^{2+}, and others) will bind in the iron site [10]. Fe^{2+} is tightly bound in the resting protein with a K_d of 2.5×10^{-8} M. In the presence of substrate, the iron is extremely tightly bound, having a $K_d < 10^{-11}$ M, and cannot be removed even by incubation with EDTA [10,22]. PDO is rather substrate-specific, activating only phthalate or aromatics with vicinal anionic groups. Although PDO with the Rieske site in the reduced state can oxygenate phthalate in the presence of O_2, PDR is required for efficient catalysis; other reductases tested with this enzyme are ineffective. It has been suggested that PDR not only donates electrons to the oxygenase, but also interacts with PDO in some way to increase the efficiency of oxygenation [10].

Several spectroscopic studies have been performed on this enzyme, including resonance Raman [23,24], electron-nuclear double resonance (ENDOR) [22,25], extended X-ray absorption fine structure (EXAFS) [26], and X-ray absorption near edge spectroscopy (XANES) [27], but the thrust of those studies has been to investigate the nature of the Rieske site. Much less work has been done on the mononuclear ferrous site, which is more difficult to access spectroscopically. EXAFS studies have been performed on the Zn- and Co-substituted enzyme to probe the non-heme iron site; these studies found that the metal coordination sphere contains only low Z ligands (oxygen and nitrogen). Co XANES on the metal-substituted enzyme provided the first experimental evidence of changes at this site due to the presence or absence of substrate [27]

Because PDO contains two metal centers, the mononuclear non-heme Fe^{2+} and the binuclear [2Fe–2S] Rieske cluster, it is difficult to obtain spectroscopic information directly on the native mononuclear ferrous site. The Rieske center has intense S to Fe charge transfer transitions which dominate the absorption spectrum and a characteristic electron paramagnetic resonance (EPR) signal in the catalytically active reduced state. In contrast, the non-heme Fe^{2+} site is EPR-silent due to zero-field-splitting and relaxation effects, and exhibits no intense ligand-to-Fe charge transfer transitions. However, there are ferrous d–d ligand field transitions which are weak in absorption, but which can be seen by circular dichroism (CD) and magnetic circular dichroism (MCD) spectroscopies. Furthermore, the MCD intensity is inversely proportional to the absolute temperature (C-term behavior); therefore at low temperatures, MCD is a powerful tool for probing paramagnetic non-heme ferrous sites. In its reduced and catalytically-active form, the Rieske site contains one high-spin ferric iron (ligated to the two Cys residues) and one high-spin ferrous iron (ligated to the two His residues), [Fe^{III}–Fe^{II}], which are antiferromagnetically coupled to produce a paramagnetic, MCD C-term active, S = 1/2 ground state [22]. In its oxidized form, the Rieske site contains two high-spin ferric irons, [Fe^{III}–Fe^{III}], which are antiferromagnetically coupled to produce an S = 0 ground state that is MCD C-term inactive. Thus, low-temperature MCD studies on phthalate dioxygenase which has the Rieske site oxidized will provide access to those spectral features arising from the native mononuclear Fe^{2+} site. In particular, the near-infrared (NIR) region of the MCD spectrum probes the spin-allowed d–d ligand field transitions of the ferrous site and gives information directly related to the site coordination number and geometry.

Studies on high-spin Fe^{2+} model compounds have shown ([2] and unpublished data) that distorted octahedral six-coordinate sites exhibit two MCD bands centered at ~10 000 cm^{-1} and split by ~2000 cm^{-1} for predominantly oxygen and nitrogen ligation; square

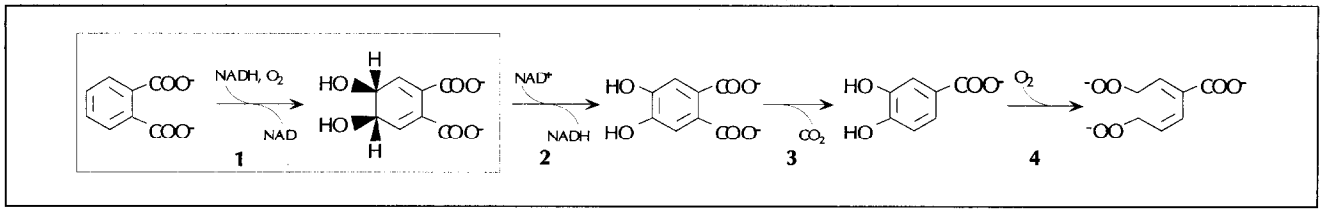

Fig. 1. The biodegradation pathway of phthalate. In step 1, phthalate is dihydroxylated to form the dihydrodiol, which is dehydrogenated in step 2 to form 4,5-dihydroxyphthalate. This is decarboxylated in step 3 to produce protocatechuate, followed by cleavage of the benzene ring in step 4 (catalyzed by protocatechuate dioxygenase to produce β-carboxy-*cis*-*cis*-muconate). PDO catalyzes the first of these steps (box) in the presence of PDR, NADH and O_2.

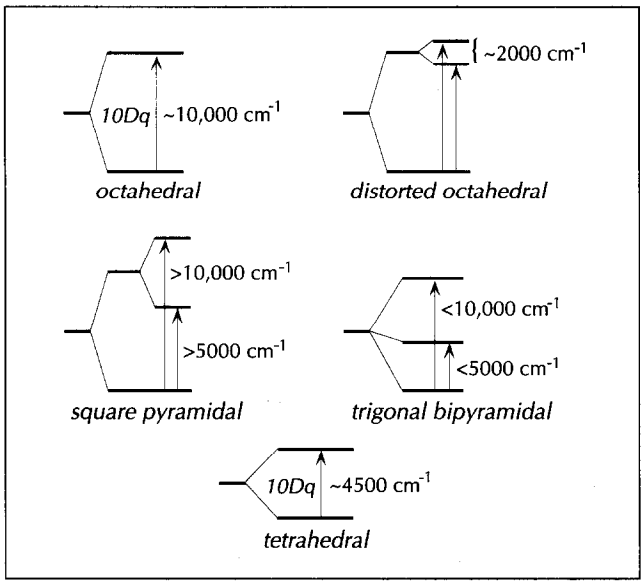

Fig. 2. Splitting pattern of the d-orbitals for different ferrous coordination environments. Arrows indicate observed ligand field transitions.

pyramidal five-coordinate sites generally display one band at ~10 000 cm^{-1} and one at ~5000 cm^{-1}, whereas these two bands are shifted to lower energy for trigonal bipyramidal coordination. Tetrahedral four-coordinate sites display one to two bands in the region of 4000 cm^{-1} to 6500 cm^{-1}, depending on ligand type and distortion (Fig. 2). Using this methodology, the coordination environment at an iron center can be determined from NIR MCD spectra, and the effects of exogenous ligand binding to a non-heme Fe^{2+} center can be directly probed.

In the course of this research, a study appeared which applied this methodology to investigate substrate binding to the non-heme ferrous site in phthalate dioxygenase [28]. In the present study, we have extended those results to include the temperature-independent contributions of the Rieske center to the MCD spectra through parallel studies on the apoprotein (defined as the enzyme with the Rieske center intact but devoid of mononuclear non-heme Fe^{2+}) and the effects of exogenous ligand binding to the ferrous site in the Fe^{2+}-reconstituted enzyme (referred to as FePDO). We have also obtained new low-energy NIR MCD data on both the oxidized and the reduced [2Fe–2S] Rieske sites in the apoenzyme. In addition to demonstrating that the presence of substrate changes the six-coordinate ferrous site in the resting enzyme to two different five-coordinate substrate-bound species, our results show that azide binds both to the resting enzyme and to the enzyme in the presence of substrate. The latter binding constant is two orders of magnitude smaller than that for the resting enzyme, indicating the presence of a steric interaction between azide and substrate. These results imply that the oxygen binding site on the non-heme Fe^{2+} is in close proximity with the aromatic ring of the substrate so that the iron–O_2 intermediate and substrate are well positioned for product formation. These exogenous ligand binding results help provide molecular-level mechanistic insight into this class of non-heme ferrous enzymes.

Results

Resting enzyme

Although the [2Fe–2S] Rieske site in the enzyme samples is oxidized with a diamagnetic S = 0 ground state, one cannot assume that there is no low-temperature MCD intensity due to these sites. Although an S = 0 ground state cannot show C-term intensity, there could be temperature-independent B-term MCD intensity resulting from field-induced mixing of electronic states [29]. Since the B-term intensity is proportional to the absorption intensity, which is quite high for Rieske centers, it can make a significant contribution. Additionally, any small paramagnetic impurity in the apoprotein samples would show low-temperature MCD intensity and could mask weak ligand field features originating from the non-heme Fe^{2+} center. Therefore, to obtain accurate spectra for just the ferrous active site in PDO, we recorded the MCD spectra of both an FePDO sample and an apoPDO sample from the same batch of stock protein under identical conditions. Fig. 3a

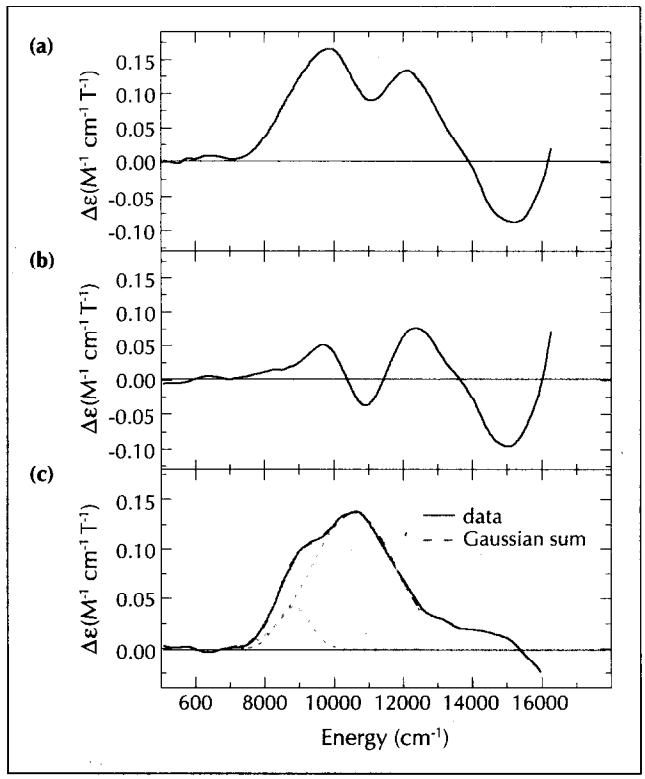

Fig. 3. Low-temperature MCD spectra of FePDO and apoPDO. **(a)** MCD spectrum of FePDO with one equivalent of Fe^{2+}. **(b)** MCD spectrum of the corresponding apoPDO. **(c)** Difference MCD spectrum of FePDO minus apoPDO; the red dashed line shows the best Gaussian fit to the data (the green lightly-dashed lines show individual Gaussian components). Spectra were recorded at 5 K and 7.0 T with the natural CD (0.0 T) spectra at 5 K subtracted. Samples were ~1.8 mM in active sites in 60 % (v/v) glycer(ol-d_3)/100 mM HEPES buffer (pD 8.0); path lengths were 0.3 cm.

shows the data for FePDO with one molar equivalent of ferrous ion added relative to active sites; Fig. 3b shows the MCD spectrum of the corresponding apoPDO sample on the same scale. It can be seen that the apoprotein does in fact show low-temperature MCD intensity and that, for these samples, the apoPDO intensity is comparable to that of the resting enzyme.

The difference spectrum obtained by subtracting the low-temperature MCD spectrum of the apoprotein from that of the resting enzyme (Fig. 3c) shows two peaks which can be Gaussian fit with bands at 8850 cm^{-1} (700 cm^{-1}) and 10 580 cm^{-1} (1700 cm^{-1}), where the half-widths at half-maximum (HWHM) values are given in parentheses. These two peaks, centered at ~9700 cm^{-1} and split by ~1700 cm^{-1}, are indicative of a six-coordinate Fe^{2+} site, an assignment which is in agreement with Co XANES results [27]. In addition to showing the presence of this six-coordinate iron site, previous MCD studies [28] on this enzyme have also shown the presence of a third band at ~12 000 cm^{-1}. It was postulated that this additional band was due to the presence of a five-coordinate iron species which becomes the predominant species when substrate is added. When the apoPDO spectrum is taken into account and subtracted from the FePDO data, however, there is no longer any indication of an additional band around 12 000 cm^{-1}, nor is there any indication of a low-energy band in the ~5000 cm^{-1} region which would also arise from a five-coordinate species. (The non-zero MCD intensity observed at >13 000 cm^{-1} in Fig. 3c results from the apoenzyme MCD subtraction; our studies on other PDO/apoPDO samples show no intensity in this region. For consistency, all spectra presented in this paper were collected on samples prepared from the same apoprotein stock.) It should be noted that when one half-molar equivalent of ferrous ion (relative to active sites) was added to the apoenzyme, the resulting FePDO-minus-apoPDO spectrum showed identical results to those seen for stoichiometric addition of Fe^{2+}, but with half the intensity. We therefore conclude that the resting enzyme exists in a clean form as a single distorted octahedral six-coordinate species which gives rise to the two bands seen in Fig. 3c.

Azide binding to resting enzyme

The effect of exogenous ligand binding to the ferrous active site was probed by adding different concentrations of azide to the resting enzyme and monitoring changes in the low-temperature MCD spectra. Room temperature CD studies were not feasible as the CD features from the Rieske site completely dominate the spectrum. Fig. 4a presents the low-temperature MCD spectrum of FePDO plus 40 molar equivalents of azide compared with the spectrum of the resting enzyme, and Fig. 4b shows the MCD spectrum of FePDO plus 160 molar equivalents of azide. The addition of azide to the apoprotein caused some perturbation in the high-energy region of the MCD spectrum, so the low-temperature MCD spectra of matched apoPDO samples (no azide, 40x azide, or 160x azide) were subtracted from the corresponding

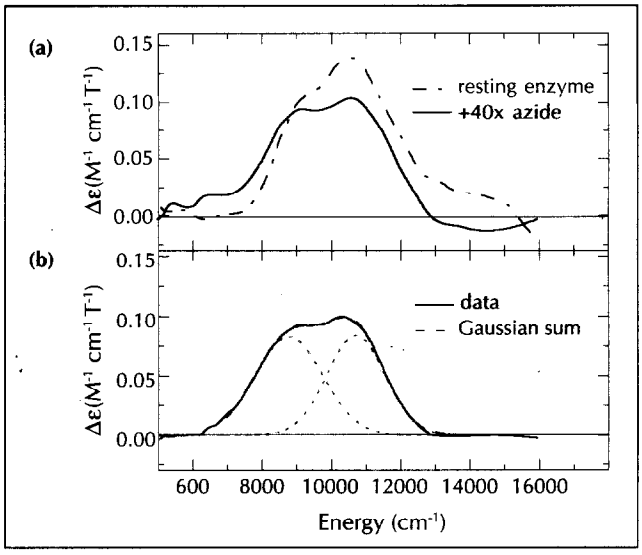

Fig. 4. Low-temperature MCD spectra of FePDO in the presence and absence of azide. **(a)** MCD spectra of FePDO + 40x azide (solid line) and resting FePDO (dashed line). **(b)** MCD spectrum of FePDO + 160x azide; the red dashed line shows the best Gaussian fit to the data (the green lightly-dashed lines show individual Gaussian components). Spectra were recorded at 5 K and 7.0 T with the 5 K, 0.0 T spectra subtracted, followed by subtraction of the 5 K, 7.0 T – 0.0 T spectrum of the matching apoPDO sample (no azide, 40x azide, or 160x azide). Samples were ~1.7 mM in active sites.

FePDO spectra. From Fig. 4a, it is clear that the FePDO-azide spectrum is not the same as the resting FePDO spectrum, demonstrating that the addition of azide perturbs the ferrous site.

Gaussian fitting of the FePDO + 160x azide spectrum results in the identification of two peaks located at 8810 cm^{-1} (1380 cm^{-1}) and 10 740 cm^{-1} (1190 cm^{-1}), with HWHM values in parentheses. These peaks are centered at ~9800 cm^{-1} and are split by 1930 cm^{-1}, indicating a six-coordinate Fe^{2+} site which is different from the six-coordinate Fe^{2+} site in the resting enzyme. The peak intensities of the apo-corrected FePDO + 40x azide spectrum are nearly identical to those of the FePDO + 160x azide spectrum, indicating that there is little change in the amount of bound azide between 40-fold excess and 160-fold excess azide. From these data, azide binding appears to be ~95 % complete by the addition of 40x azide and a binding constant can be estimated as K_B(azide to resting enzyme) = 300 ± 100 M^{-1}. Comparison of the Gaussian fit of the FePDO + 160x azide MCD spectrum to that of resting FePDO shows that the two bands in the enzyme–azide spectrum have a wider splitting and a different intensity ratio between peaks than was observed for the resting enzyme. Therefore, we conclude that azide binds to the ferrous site by replacing one endogenous iron ligand to produce a new six-coordinate species.

Substrate binding to resting enzyme

The MCD spectrum of FePDO with a five-fold molar excess of phthalate added is shown in Fig. 5. The top spectrum shows the uncorrected 5 K, 7.0 T data, and the

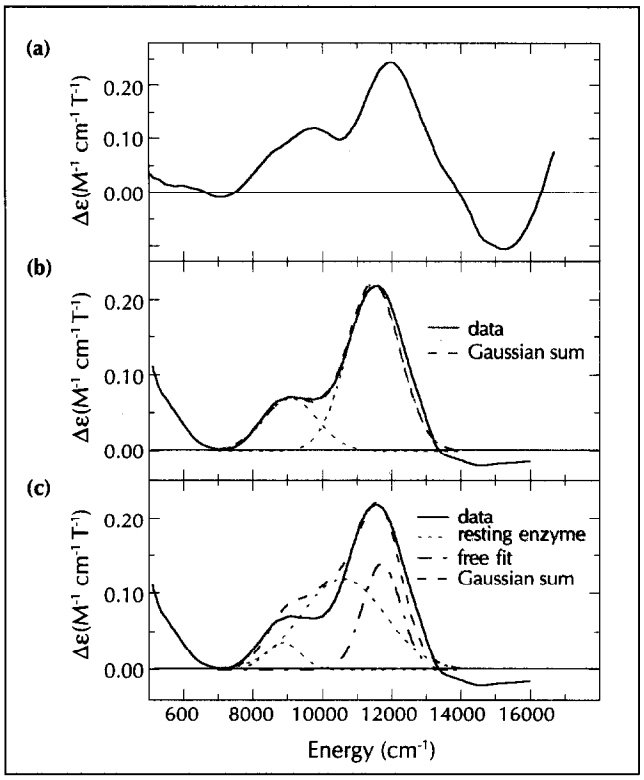

Fig. 5. Low-temperature MCD spectra of FePDO in the presence of substrate. **(a)** MCD spectrum (5 K, 7.0 T–0.0 T) of FePDO + 5x phthalate, ~1.7 mM in active sites. **(b)** MCD spectrum of FePDO + 5x phthalate minus the spectrum of apoPDO + 5x phthalate; the red dashed line shows the best Gaussian fit to the data (the green lightly-dashed lines show individual Gaussian components). **(c)** Simulation (dashed line) of plot B using the two peaks from the best fit of resting FePDO and allowing a third free-floating peak to fit the rest of the spectrum.

middle spectrum includes subtraction of the low-temperature MCD of apoPDO + 5x phthalate. Given the protein concentrations of the these samples, a five-fold excess of phthalate amounts to more than 25x K_d of phthalate ($K_d \approx 3 \times 10^{-4}$ M [28]), providing a saturating quantity of substrate. When FePDO + 10x phthalate samples were investigated, the relative MCD intensity ratios between the peaks in Fig. 4b remained the same as for 5x phthalate samples, again indicating saturating conditions at five-fold excess phthalate.

The apoenzyme-subtracted MCD spectrum of FePDO + substrate (Fig. 5b) shows the presence of three peaks: one low-energy band at <5000 cm^{-1} and two high-energy bands which have been Gaussian-fit to lie at 9070 cm^{-1} (1100 cm^{-1}) and 11 460 cm^{-1} (1070 cm^{-1}), with HWHM values given in parentheses. Because three distinct peaks are observed in the ferrous d–d region of the MCD spectrum, there must be at least two species present to give rise to these features. Based on the methodology we developed [2], the low-energy peak must originate from either a four- or five-coordinate ferrous species. If the low-energy band were one component of a five-coordinate spectrum, we would predict square pyramidal geometry and expect a high-energy band around 10 000–12 000 cm^{-1}; experimentally a band is observed at 11 460 cm^{-1}. Earlier MCD studies [28] which assigned the binary enzyme–substrate complex to be predominantly five-coordinate also observed two peaks at <5000 and ~12 000 cm^{-1}. Therefore, in agreement with earlier work, we assign the lowest and highest energy bands in Fig. 4b as arising from one square pyramidal five-coordinate substrate-bound species.

It has been postulated that the MCD intensity in the 9000–10 000 cm^{-1} region was due to residual six-coordinate resting enzyme which did not change upon substrate binding at saturating concentrations [28]. This explanation, however, was based on data from which the apoPDO MCD spectrum had not been subtracted. Without apoprotein subtraction, the enzyme–substrate data in Fig. 5a does show two features in the ~10 000 cm^{-1} region which look very much like the resting enzyme data. When the low-temperature MCD of an apoPDO + 5x phthalate sample is subtracted, however, only the one band at 9070 cm^{-1} remains (Fig. 5b). To further evaluate whether this remaining band might arise from residual resting enzyme, a simulation of the data was performed using the Gaussian-fitting results of resting FePDO. The band positions, HWHM, and relative intensities of the two peaks used to fit the resting enzyme data were used to fit the low-energy side of the 9 070 cm^{-1} band, and a third free-floating peak was included to fit the remainder of the spectrum. The resulting Gaussian sum for this simulation (Fig. 5c, dashed spectrum) does not fit the data, indicating that the 9070 cm^{-1} band does not originate from residual resting sites, but rather originates from a second Fe^{2+}-coordination environment of the substrate-bound enzyme.

The 9070 cm^{-1} feature could be assigned as one component of a trigonal bipyramidal five-coordinate Fe^{2+} spectrum, in which case a second, lower-energy band would exist below the range of the NIR CD/MCD instrument. Alternatively, this feature could be assigned as one component of a distorted octahedral six-coordinate Fe^{2+} spectrum, in which case a second band should be present at 1000–2000 cm^{-1} higher energy. Based on the Co XANES results on the metal-substituted enzyme which showed that the absolute integrated pre-edge intensity of oxidized-Rieske protein plus substrate was consistent with a pure five-coordinate mononuclear Fe^{2+} site [27], it is reasonable to assign the 9070 cm^{-1} band in the MCD spectrum as originating from a trigonal bipyramidal five-coordinate substrate-bound species which has a different ligand field environment from that of the predominant square pyramidal five-coordinate species responsible for the <5000 and 11 460 cm^{-1} peaks. It should be noted that substrate analog studies [10] indicate that phthalate does not bind directly to the iron, but rather induces a conformational change at the ferrous site through hydrogen bonding between the protein residues near the metal center and the two vicinal carboxy groups of the substrate. Therefore, given saturating concentrations of phthalate,

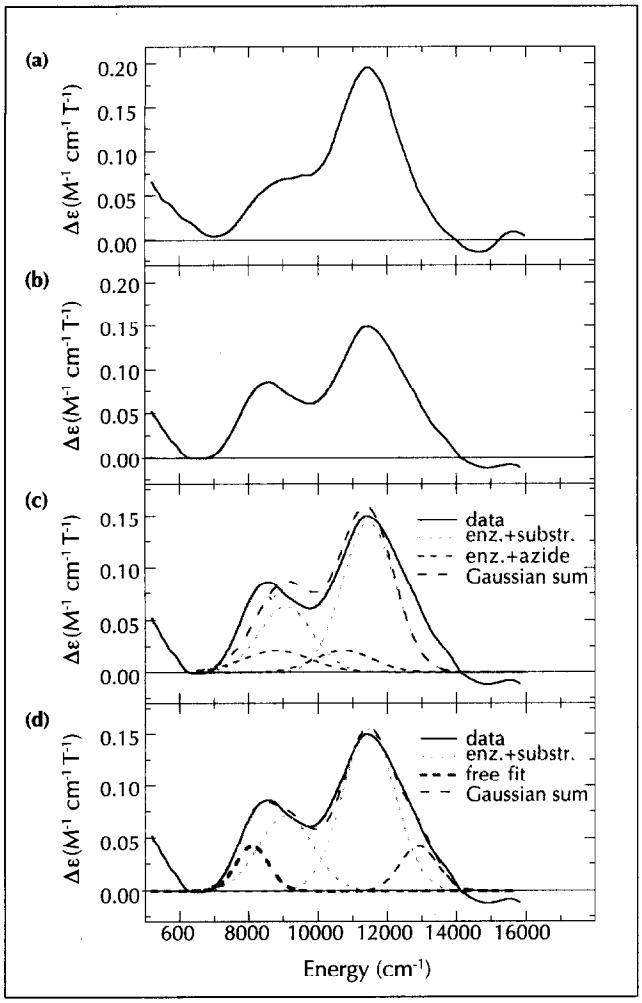

Fig. 6. Low-temperature MCD spectra for enzyme–substrate complexes in the presence of varying amounts of azide. **(a)** MCD spectrum of FePDO + 5x phthalate + 40x azide. **(b)** MCD spectrum of FePDO + 5x phthalate + 120x azide. Spectra were recorded at 5 K, 7.0 T with the 5 K, 0.0 T spectra and apoPDO spectra subtracted; samples were ~1.6 mM in active sites. **(c)** Simulation (dashed line) of plot B using the two peaks from the best fit of enzyme–substrate data and the two peaks from the best fit of FePDO + 160x azide (see text). **(d)** Simulation (dashed line) of plot B using the two peaks from the best fit of enzyme–substrate data and allowing for additional free-floating peaks to fit the rest of the spectrum.

the substrate binds fully to the enzyme and perturbs the mononuclear ferrous site by causing the displacement of one ligand, lowering the coordination number of the iron from six in the resting form to five in the two different substrate-bound species.

Azide binding to the enzyme–substrate complex

In parallel with the exogenous ligand binding study on resting FePDO, we performed an investigation of exogenous ligand binding effects on the enzyme–substrate complex by adding azide to FePDO + 5x phthalate samples. It should be noted that under standard assay conditions [10], an azide:Fe^{2+} ratio of ~3500:1 caused ~23 % loss of activity, indicating that azide causes weak inhibition. Fig. 6a shows the low-temperature MCD of FePDO + 5x phthalate to which a 40-fold molar excess of azide has been added; the spectrum of the corresponding apoPDO + 5x phthalate + 40x azide has been subtracted. Fig. 6b presents the apoenzyme-corrected MCD spectrum of the same FePDO + 5x phthalate sample, but now with 120x azide added. Comparison of the spectrum of FePDO + 5x phthalate + 40x azide (Fig. 6a) with that of FePDO + 5x phthalate with no azide (Fig. 5b) indicates that there are no changes in the MCD peak positions when 40x azide has been added and only a slight loss of intensity (< 10 %) is observed in the high-energy peak at 11 460 cm^{-1}. The addition of 120x azide produces more of a change in the spectrum: the low-energy peak positions have shifted and there is now ~25 % less intensity in the high-energy band. This loss of intensity at 11 460 cm^{-1} indicates that some of the square pyramidal five-coordinate Fe^{2+} sites giving rise to that band have been changed into another species with different spectral features and therefore a different coordination environment. Through monitoring the loss of the 11 460 cm^{-1} intensity and assuming that the amount of square pyramidal species lost is a lower limit on the amount of new species formed, an azide binding constant can be estimated as $K_B = 2 \pm 1\ M^{-1}$ for azide binding to the enzyme–substrate complex. It should be noted that there is clearly a mixture of species contributing to the spectrum in Fig. 6b which makes definitive analysis more difficult.

One possible effect of azide binding to FePDO + 5x phthalate is that azide could displace substrate and bind to the non-heme iron to form the six-coordinate FePDO-azide complex observed when azide was added to resting enzyme, as in Fig. 4b. To evaluate this possibility, a simulation of the data was performed using the Gaussian results of the FePDO + 5x phthalate spectrum (Fig. 5b) and the FePDO + 160x azide spectrum (Fig. 4b): the two enzyme–substrate bands were fixed in peak position and HWHM, but not in relative intensity since the two different five-coordinate species giving rise to these peaks may be perturbed differently by the addition of azide; the two enzyme–azide bands were fixed in peak position, HWHM, and relative intensity. To approximate the amount of enzyme–azide species that may be formed, the total intensity from the enzyme–azide bands was held at 25 % of the full intensity from Fig. 4b. Since the best Gaussian sum resulting from this simulation (Fig. 6c, dashed line) does not fit the data, particularly in the low-energy region, it can be concluded that the addition of azide does not displace substrate to form the resting enzyme–azide species, but rather that azide binds to form a ternary enzyme–substrate–azide complex.

A second simulation of the data (Fig. 6d) was performed using fixed peak positions and HWHM for the enzyme–substrate bands and allowing for additional free-floating peaks, corresponding to the ternary complex, to obtain the best fit to the data. Although the Gaussian components of the simulation may not be meaningful at high energy where slightly mismatched apoprotein

subtractions can affect the data, the low-energy region of the simulation clearly shows that a third peak, centered at ~8100 cm^{-1}, is required to fit the spectrum. This additional peak presumably originates from the ternary enzyme–substrate–azide complex and is positioned in the energy region of either a trigonal bipyramidal five-coordinate or a distorted octahedral six-coordinate ferrous species. It is possible that the trigonal bipyramidal component of the enzyme–substrate species can bind azide to form a ternary complex with azide replacing one endogenous ferrous ligand. Unfortunately, it is not clear from the data whether the trigonal bipyramidal enzyme–substrate component reacts with azide because of the mixture of species present. It is, however, clear that the square pyramidal enzyme–substrate component binds azide to form a ternary complex (*vide supra*), and it is reasonable for azide to bind in the open coordination position available, thus forming a distorted octahedral six-coordinate ternary complex. If the ~8100 cm^{-1} peak is one component of a six-coordinate spectrum, then a second peak should lie at ~10 000 cm^{-1}, an energy region which is obscured by the peaks from the non-azide-bound enzyme–substrate complexes. For a six-coordinate species, the ~8100 cm^{-1} band is to lower energy than would be expected for typical oxygen and nitrogen ligation [2]. This effect would indicate a lower ligand field environment at the ferrous site resulting from azide binding weakly to the iron due to either a long Fe-N(azide) bond or reduced sigma overlap because of the azide orientation. The fact that azide binds weakly to the mononuclear iron appears to be due to the presence of substrate in close proximity which would sterically interfere with the open coordination site.

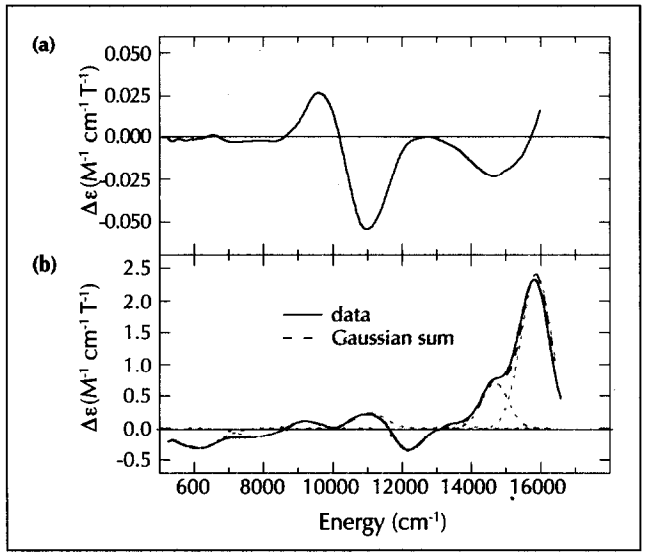

Fig. 7. Low-temperature NIR MCD spectra of reduced and oxidized Rieske sites. **(a)** 100 K MCD spectrum of apoPDO with the Rieske site oxidized. **(b)** 5 K MCD spectrum of apoPDO with the Rieske site reduced; the red dashed line shows the best Gaussian fit to the data (the green lightly-dashed lines show individual Gaussian components). Spectra were recorded at 7.0 T with the 0.0 T spectra subtracted; sample concentrations were ~1.8 mM in Rieske sites.

The Rieske site

In the course of recording MCD spectra of apoPDO for subtraction purposes, clean spectra of the [2Fe–2S] Rieske site in the apoenzyme were collected. Although this type of iron–sulfur center has been well studied by several other spectroscopic techniques, only the room temperature visible CD and MCD of a Rieske site have been recorded to date [30–32]. Therefore, we present low-temperature NIR MCD spectra of both the oxidized and reduced Rieske sites (Fig. 7). It should be noted that the oxidized Rieske spectrum presented in Fig. 7a was recorded at 100 K because small paramagnetic impurities in the sample gave rise to weak temperature-dependent signals at low temperature while only the intrinsic oxidized S = 0 Rieske features appear at higher temperatures. The observed MCD $\Delta\varepsilon$ values from the oxidized [Fe^{III}–Fe^{III}] site are one to two orders of magnitude weaker than the $\Delta\varepsilon$ values from the reduced [Fe^{III}–Fe^{II}] site. Furthermore, there are no common features between the spectra of the oxidized and reduced Rieske sites.

The MCD spectrum of the reduced Rieske site exhibits several bands in the low-energy region where iron ligand field transitions occur (Fig. 7b). Comparison of the MCD features arising from the reduced Rieske center with the MCD features from reduced [2Fe–2S] ferredoxin centers would be interesting as a probe of different spectral features due to the His perturbation in the Rieske site, but MCD spectra of reduced [2Fe–2S] ferredoxin centers in this low-energy region are not available. There are, however, both NIR MCD and polarized absorption data available on monomeric high-spin ferrous tetrathiolate ($Fe(SR)_4^{2-}$) [33] and high-spin ferric tetrathiolate ($Fe(SR)_4^{-}$) [34] model complexes, each of which can be used as a starting point for the two halves of the reduced Rieske dimer. Based on the tetrathiolate model data, ferrous spin-allowed ligand field transitions should be observable in the <7000 cm^{-1} region and ferric spin-forbidden ligand field transitions in the 7000–12 000 cm^{-1} region of the NIR spectrum for tetrahedral thiolate complexes. One ferrous ligand field transition for $Fe(SR)_4^{2-}$ was observed at 4600 cm^{-1} with no other MCD bands observable until >14 000 cm^{-1}, where the ferrous spin-forbidden ligand field transitions occur [33].

Using these model data as a guide, the MCD band observed at lowest energy (~6100 cm^{-1}) in Fig. 7b can be assigned as a ferrous spin-allowed ligand field transition, and the next observed band (~7800 cm^{-1}) can be assigned as either another ferrous spin-allowed transition or the first of several ferric spin-forbidden ligand field transitions originating from the Fe^{III} site of the Rieske center. This assignment of the 6100 cm^{-1} band demonstrates that 10Dq in Fig. 2, bottom, for the reduced Rieske site is significantly higher than for a tetrahedral ferrous tetrathiolate center. A higher 10Dq is consistent with the fact that the Rieske Fe^{II} site has two His ligands in place of thiolate ligands, as in the model and reduced ferredoxins, since imidazole has a stronger ligand field

than thiolate. Additionally, because the Rieske Fe^{II} site is more distorted than the model tetrathiolate compound, having at most C_{2v} symmetry compared to D_{2d} or S_4 symmetry in the model, the $^5T_2$ excited state should have a larger low-symmetry splitting for the Rieske site and ligand field transitions should occur at higher energy, as observed. The increased 10Dq and low-symmetry splitting on the Fe^{II} of the reduced Rieske site relative to the tetrathiolate model means that the d-orbital containing the extra electron is lowered and that there is an increased ligand field stabilization energy of the ferrous center which contributes to the higher reduction potential of the Rieske clusters.

Discussion

The effects of substrate binding to the mononuclear ferrous active site in phthalate dioxygenase have initially been probed by X-ray absorption [26] and magnetic circular dichroism [28] spectroscopies. In agreement with these studies, our MCD results show that the resting enzyme contains a six-coordinate Fe^{2+} site which changes upon substrate binding to a five-coordinate site. Furthermore, our data show that the resting enzyme contains only one six-coordinate species and that the binary enzyme–substrate complex actually consists of a mixture of two different five-coordinate substrate-bound species, one approximately square pyramidal and one more distorted toward trigonal bipyramidal, with no residual six-coordinate site present. It is interesting to compare these results with substrate-binding studies performed on other mononuclear non-heme ferrous enzymes. Like PDO, soybean lipoxygenase-1 (SLO-1) and metapyrocatechase are both air-stable in their resting ferrous states. Resting SLO-1 contains a mixture of five- and six-coordinate Fe^{2+} sites and is shifted to the pure six-coordinate species upon the addition of substrate [35]. Resting metapyrocatechase contains a five-coordinate iron site, and substrate addition results in the bidentate binding of catechol (replacing two endogenous ligands) to produce a different five-coordinate species [36]. Thus for SLO-1 and metapyrocatechase, the iron coordination number either increases or remains the same. PDO therefore appears to be the first mononuclear non-heme ferrous enzyme found to exhibit a decrease in coordination number upon substrate addition, where substrate binds to the protein pocket near the ferrous center and induces a conformational change at the iron site.

Although little mechanistic information is available on any of the bacterial dioxygenases, there is mechanistic information [1] on putidamonooxin (4-methoxybenzoate *O*-demethylase) (PMO), which also contains a Rieske cluster and a mononuclear non-heme ferrous active site. Unlike the bacterial dioxygenases, PMO is not highly specific with regard to substrate and can act as an external dioxygenase, a monooxygenase, or an oxidase [37]. Although resting PMO is not air-stable in the ferrous state, substrate and NO-binding studies have been performed on anaerobically-treated ferrous enzyme using EPR [37,38] and Mössbauer [39] spectroscopies. As was found for PDO, the addition of substrate perturbs the mononuclear iron site in PMO [39], though it is not yet clear whether substrate binds to the iron or causes a conformational change at the site or whether the perturbation induces a reduction in the coordination number of the Fe^{2+} center. NO-binding studies showed that NO can bind both to the resting ferrous enzyme and to the enzyme–substrate complex, in the latter case forming a ternary complex; these results are analogous to the azide-binding studies on PDO. The active form of PMO is proposed to be a ternary enzyme–substrate–O_2 complex for which the mononuclear non-heme iron is in the Fe^{2+} state. The reaction order for this system is such that substrate binds first to the mononuclear iron in its Fe^{3+} state, followed by reduction of the ferric enzyme–substrate complex to the ferrous state; molecular oxygen then reacts with the Fe^{2+} and is thought to form a ferric-peroxide intermediate which goes on to attack the aromatic ring of the substrate [37]. Although there are no detailed studies on the reaction mechanism of PDO, kinetic studies [10,40] favor a mechanism in which the substrate binds first, followed by O_2 binding and activation by the non-heme iron, as do the results on PMO.

The loss of one ligand at the active site in PDO when substrate binds may serve to produce a coordinatively unsaturated square pyramidal ferrous center which is therefore able to bind and activate oxygen for product formation. Resting FePDO with the Rieske site oxidized does not react with O_2; however, our ligand-binding studies have shown that azide will bind to the resting six-coordinate active site, changing the environment at the iron by replacing one ligand to produce a different six-coordinate site. These results demonstrate the presence of an exchangeable coordination position at the Fe^{2+} site, and it is possible that the ligand exchanged by azide is the same labile ligand which is lost upon substrate binding. It has also been shown that the addition of azide to the five-

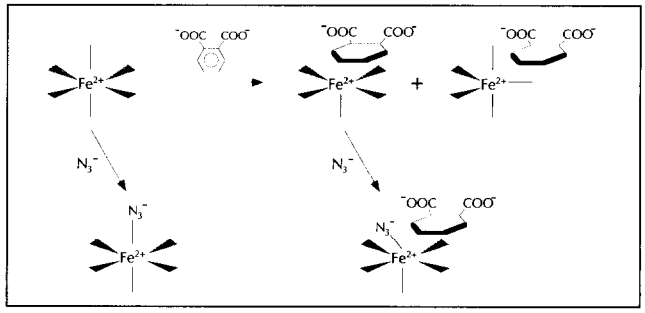

Fig. 8. Proposed changes in the mononuclear Fe^{2+} site coordination environment due to the addition of exogenous ligands and substrate. Upon substrate binding, the iron coordination changes from six-coordinate to five-coordinate, with two different five-coordinate species produced, one square pyramidal and the other more trigonal bipyramidal. The square pyramidal species is coordinatively unsaturated and can therefore bind azide or molecular oxygen. Azide binding in the absence of substrate involves exchange of one of the ligands in the resting six-coordinate site, producing a different six-coordinate species.

coordinate enzyme–substrate species does not cause the displacement of substrate, but rather produces a new ternary enzyme–substrate–azide complex. Although it is possible that a trigonal bipyramidal ternary species is formed, the enzyme–substrate–azide complex likely contains a distorted octahedral six-coordinate ferrous site with azide occupying the open coordination position available from the square pyramidal five-coordinate enzyme–substrate species.

Because the square pyramidal enzyme–substrate complex contains an open coordination site, it would be expected that small molecules should easily to bind to the ferrous site; however, the binding constant for azide coordination to the enzyme–substrate complex was found to be approximately two orders of magnitude lower than for the resting enzyme (K_B = ~2 M^{-1} versus ~300 M^{-1}). These results are again quite different from ligand binding studies on the extradiol dioxygenase metapyrocatechase, which showed that azide did not bind to the resting enzyme, but that the addition of substrate activated the iron site for azide binding [36]. The low binding constant for azide binding to the PDO enzyme–substrate complex would appear to result from a steric interaction between the substrate and azide bound to the open coordination position on the iron. Thus, using the azide binding as a model for the oxygen interaction, these results indicate that the O_2-binding site is in close proximity to the aromatic ring of the substrate, positioning the bound oxygen intermediate and substrate for product formation. The proposed changes in the coordination environment at the mononuclear Fe^{2+} active site in PDO due to exogenous ligand and substrate binding are summarized in Fig. 8.

Significance

Phthalate dioxygenase catalyzes the *cis*-dihydroxylation of phthalate and is one of several bacterial oxygenases that activate aromatics for catabolism, helping to destroy both natural and man-made toxins in the environment. Its mechanism is unknown, however, in part because the mononuclear non-heme Fe^{2+} active site in PDO has been difficult to study because of the additional presence of a [2Fe–2S] Rieske site which dominates most spectroscopies. Because the Rieske site can be rendered diamagnetic by oxidation to the [Fe^{III}–Fe^{III}] S = 0 state, however, MCD spectroscopy provides direct access to the non-heme Fe^{2+} center by selectively probing the paramagnetic ferrous center at low temperatures.

Here, we have focused on the effects of exogenous ligand binding to the active site in the resting enzyme and in the binary enzyme–substrate complex. Our results show that azide binds to the six-coordinate resting enzyme to form a new six-coordinate Fe^{2+} species, indicating the presence of an exchangeable endogenous ligand at the metal site. Furthermore, these results demonstrate that the addition of substrate to resting enzyme produces two different five-coordinate substrate-bound species with no residual six-coordinate sites present, thereby opening a coordination position for O_2 reaction. Azide was also found to bind to this binary species, forming a ternary complex, but with a much lower binding constant than was obtained for the resting enzyme, indicating that the exogenous ligand binds in close proximity to the substrate in the sterically-constrained open coordination site of the ferrous center.

These studies have provided new structural insight into substrate and exogenous ligand interactions with the non-heme Fe^{2+} site of relevance to O_2 binding and activation by this class of bioremediation enzymes. It is hoped that this study will stimulate further investigation of the mechanistic order to maximize the molecular-level detail available from these spectroscopic studies. Further, this study shows that MCD can be a powerful probe of non-heme ferrous active sites, providing insight into the mechanism of these sites and into how differences in the iron sites of different enzymes relate to differences in reactivity.

Materials and methods

All commercial reagents were used without further purification: HEPES buffer (Research Organics, Inc., Sigma), potassium hydrogen phthalate (Aldrich), EDTA (Mallinckrodt), NADH (United States Biochemical), 2,2'-dipyridyl (99+%; Aldrich), sodium azide (99 %; Aldrich), D_2O (99.9 atom % D; Aldrich, Cambridge Isotope Laboratories), glycer(ol-d_3) (98 atom % D; Aldrich, Cambridge Isotope Laboratories), sodium deuteroxide (99+ atom % D; Aldrich), and ferrous ammonium sulfate (MCB Manufacturing Chemists, Inc.).

Pseudomonas cepacia (ATCC 29424) was grown in phthalate-mineral salts medium using a 12L NBS Microgen fermentor. Phthalate dioxygenase was isolated from *P. cepacia* as previously described [10], with the exception that the final DEAE ion-exchange chromatography step was omitted. The purity of the samples in all cases was judged to be >95 % by sodium dodecyl sulfate-polyacrylamide gel electrophoresis. Mononuclear iron was removed by the addition of EDTA and 2,2'-dipyridyl, to a final concentration of 10 mM each, to the PDO samples. The samples were incubated for 15–20 h at 4 °C, followed by dialysis versus two exchanges of 0.05 M HEPES at pH 8.0. The apoPDO samples were then exchanged into 50 mM HEPES in D_2O (pD 8.0) using several dilution and ultrafiltration cycles in a Centricon-30 microconcentrator (Amicon). Apoenzyme was run through an additional Chelex-100 column in 100 mM HEPES (pD 8.0) to remove any remaining mononuclear iron. Liquid helium-temperature EPR of this apoprotein with the Rieske site oxidized showed only a slight feature at g = 4.3 (free ferric iron); anaerobic addition of excess sodium dithionite to reduce the [2Fe–2S] site produced the characteristic rhombic Rieske EPR spectrum (g = 2.02, 1.92, 1.8) [30]. Samples used for CD and MCD showed none of the rhombic EPR features, confirming that the Rieske sites were in the fully oxidized state.

EPR-checked apoPDO was exchanged into 100 mM HEPES (pD 8.0) by several dilution and ultrafiltration steps using a Centricon-50 concentrator (Amicon) and concentrated for spectroscopic conditions. Concentrations were determined by absorbance at 464 nm, using $\varepsilon = 7800\ M^{-1}cm^{-1}$ per mole of [2Fe–2S] sites [10]; therefore, all concentrations reported refer to the Rieske sites as well as the mononuclear ferrous sites (active sites). Although this enzyme is stable in air, all further sample manipulations were performed anaerobically to prevent the reaction of any unbound or dissociated ferrous iron with molecular oxygen. Concentrated apoprotein was made anaerobic by repeated cycles of evacuation and flushing with O_2-scrubbed argon. The apoPDO samples were then diluted 55–60 % (v/v) by anaerobic addition of glycer(ol-d_3). FePDO samples were made by the addition of one equivalent of a degassed stock solution of $Fe(NH_4)_2(SO_4)_2 \cdot 6H_2O$ in D_2O to the apoprotein-glycer(ol-d_3) stock solution. Phthalate was added in microliter quantities from a degassed stock solution of potassium hydrogen phthalate in D_2O, and enzyme–substrate samples were allowed to incubate at 4 °C under argon for ~12 h. Azide additions were made in microliter quantities from degassed stock solutions of sodium azide in D_2O. For samples containing both phthalate and azide, the phthalate stock was added first. Reduced Rieske samples were prepared by the anaerobic addition of excess sodium dithionite from a D_2O stock solution to the oxidized Rieske samples. Experimental measurement of the pD for sample conditions in which 160-fold excess azide had been added to resting enzyme showed that the pD did not change by more than 0.04 at room temperature.

Final PDO samples for spectroscopy were in the form of a glass with 55–60 % (v/v) degassed glycer(ol-d_3)/0.10 M HEPES buffer at pD 8.0 and were typically 1.6 mM to 2.1 mM in active sites. Samples were injected anaerobically into an argon-purged MCD cell made by compressing a 0.3-cm thick neoprene gasket between two quartz plates. Room temperature NIR CD spectroscopy (600–2000 nm) was performed on a Jasco 200D spectropolarimeter with an InSb detector. Low-temperature CD and MCD spectra were obtained using the Jasco spectropolarimeter equipped with a modified sample compartment to accommodate an Oxford Instruments Spectromag 4 superconducting magnet/cryostat (Oxford SM4-7T) and focusing optics. Depolarization of the light by the MCD protein glasses was monitored by their effect on the room temperature CD signal of a nickel (+)-tartarate solution placed before and after the sample. In all cases, the depolarization was < 5 % at 5 K. Addition of glycerol to the samples showed no significant perturbation in the room temperature CD spectra of either apoPDO or FePDO.

MCD spectra shown were recorded at 5 K unless otherwise noted and 7.0 T with the natural CD (0.0 T) subtracted. For the iron samples, the 5 K, 7.0 T–0.0 T MCD spectrum of a matched apoprotein sample was subtracted. The matched apoprotein sample came from the same degassed protein stock solution and contained the same amount of exogenous ligand(s). The MCD spectra have been smoothed by rebinning the data to reduce statistical noise. The unsmoothed data were fit with Gaussian bandshapes using a constrained nonlinear least-squares fitting procedure. Where simulations of the data were performed using the Gaussian fitting results of other spectra, the pre-assigned bands were fixed in peak position, HWHM, and relative intensities as indicated.

Acknowledgements: This research was supported by the National Institutes of Health, Grants No. GM40392 (E.I.S.) and GM43507 (W.R.E.).

References

1. Feig, A.L. & Lippard, S.J. (1994). Reactions of non-heme iron(II) centers with dioxygen in biology and chemistry. *Chem. Rev.* **94**, 759–805.
2. Solomon, E.I. & Zhang, Y. (1992). The electronic structures of active sites in non-heme iron enzymes. *Accounts Chem. Res.* **25**, 343–352.
3. Que, L., Jr. (1980). Non-heme iron dioxygenases: structure and mechanism. *Struct. Bonding* **40**, 39–72.
4. Veldink, G.A. & Vliegenthart, J.F.G. (1984). Lipoxygenases, nonheme iron-containing enzymes. *Adv. Inorg. Biochem.* **6**, 139–161.
5. Nozaki, M. (1979). Oxygenases and dioxygenases. *Top. Curr. Chem.* **78**, 145–186.
6. Lipscomb, J.D. & Orville, A.M. (1992). Mechanistic aspects of dihydroxybenzoate dioxygenases. In *Metal Ions in Biological Systems.* (Sigel, H. & Sigel, A., eds), pp. 243–298, Marcel Dekker, New York.
7. Dix, T.A. & Benkovic, S.J. (1988). Mechanism of oxygen activation by pteridine-dependent monooxygenases. *Accounts Chem. Res.* **21**, 101–107.
8. Salowe, S.P., Marsh, E.N. & Townsend, C.A. (1990). Purification and characterization of clavaminate synthase from *Streptomyces clavuligerus*: an unusual oxidative enzyme in natural product biosynthesis. *Biochemistry* **29**, 6499–6508.
9. Ruettinger, R.T., Griffith, G.R. & Coon, M.J. (1977). Characterization of the ω-hydroxylase of *Pseudomonas oleovorans* as a nonheme iron protein. *Arch. Biochem. Biophys.* **183**, 528–537.
10. Batie, C.J., LaHaie, E. & Ballou, D.P. (1987). Purification and characterization of phthalate oxygenase and phthalate oxygenase reductase from *Pseudomonas cepacia*. *J. Biol. Chem.* **262**, 1510–1518.
11. Stubbe, J. & Kozarich, J.W. (1987). Mechanisms of bleomycin-induced DNA degradation. *Chem. Rev.* **87**, 1107–1136.
12. Hecht, S.M. (1986). The chemistry of activated bleomycin. *Accounts Chem. Res.* **19**, 383–391.
13. Crutcher, S.E. & Geary, P.J. (1979). Properties of the iron–sulphur proteins of the benzene dioxygenase system from *Pseudomonas putida*. *Biochem. J.* **177**, 393–400.
14. Yamaguchi, M. & Fujisawa, H. (1980). Purification and characterization of an oxygenase component in benzoate 1,2-dioxygenase system from *Pseudomonas arvilla* C-1. *J. Biol. Chem.* **255**, 5058–5063.
15. Ensley, B.D. & Gibson, D.T. (1983). Naphthalene dioxygenase: purification and properties of a terminal oxygenase component. *J. Bacteriol.* **155**, 505–511.
16. Sauber, K., Fröhner, C., Rosenberg, G., Eberspächer, J. & Lingens, F. (1977). Purification and properties of pyrazon dioxygenase from pyrazon-degrading bacteria. *Eur. J. Biochem.* **74**, 89–97.
17. Gibson, D.T., Yeh, W.K., Liu, T.N. & Subramanian, V. (1982). Toluene dioxygenase: a multicomponent enzyme system from *Pseudomonas putida*. In *Oxygenases and Oxygen Metabolism.* (Nozaki, M., Yamamoto, S., Ishimura, Y., Coon, M.J., Ernster, L. & Estabrook, R.W., eds), pp. 51–62, Academic Press, New York.
18. Markus, A., Krekel, D. & Lingens, F. (1986). Purification and some properties of component A of the 4-chlorophenylacetate 3,4-dioxygenase from *Pseudomonas* species strain CBS. *J. Biol. Chem.* **261**, 12883–12888.
19. Brunel, F. & Davison, J. (1988). Cloning and sequencing of *Pseudomonas* genes encoding vanillate demethylase. *J. Bacteriol.* **170**, 4924–4930.
20. Bernhardt, F.H., Heymann, E. & Traylor, P.S. (1978). Chemical and spectral properties of putidamonooxin, the iron-containing and acid-labile-sulfur-containing monooxygenase of a 4-methoxybenzoate *O*-demethylase from *Pseudomonas putida*. *Eur. J. Biochem.* **92**, 209–223.
21. Correll, C.C., Batie, C.J., Ballou, D.P. & Ludwig, M.L. (1992). Phthalate dioxygenase reductase: a modular structure for electron transfer from pyridine nucleotides to [2Fe–2S]. *Science* **258**, 1604–1610.
22. Gurbiel, R.J., *et al.*, & Ballou, D.P. (1989). Electron-nuclear double resonance spectroscopy of ^{15}N-enriched phthalate dioxygenase from *Pseudomonas cepacia* proves that two histidines are coordinated to the [2Fe–2S] Rieske-type clusters. *Biochemistry* **28**, 4861–4871.
23. Kuila, D., Fee, J.A., Schoonover, J.R., Woodruff, W.H., Batie, C.J. & Ballou, D.P. (1987). Resonance Raman spectra of the [2Fe–2S] clusters of the Rieske protein from *Thermus* and phthalate dioxygenase from *Pseudomonas*. *J. Am. Chem. Soc.* **109**, 1559–1561.
24. Kuila, D., *et al.*, & Woodruff, W.H. (1992). Resonance Raman studies of Rieske-type proteins. *Biochim. Biophys. Acta* **1140**, 175–183.
25. Cline, J.F., Hoffman, B.M., Mims, W.B., LaHaie, E., Ballou, D.P & Fee, J.A. (1985). Evidence for N coordination to Fe in the [2Fe–2S] clusters of *Thermus* Rieske protein and phthalate dioxygenase from *Pseudomonas*. *J. Biol. Chem.* **260**, 3251–3254.

26. Tsang, H.T., Batie, C.J., Ballou, D.P. & Penner-Hahn, J.E. (1989). X-ray absorption spectroscopy of the [2Fe–2S] Rieske cluster in *Pseudomonas cepacia* phthalate dioxygenase. Determination of core dimensions and iron ligation. *Biochemistry* **28**, 7233–7240.
27. Penner-Hahn, J.E. (1989). X-ray absorption spectroscopy of *Pseudomonas cepacia* phthalate dioxygenase. *Basic Life Sci.* **51**(Synchrotron Radiation in Structural Biology), 177–186.
28. Gassner, G.T., Ballou, D.P., Landrum, G.A. & Whittaker, J.W. (1993). Magnetic circular dichroism studies on the mononuclear ferrous active site of phthalate dioxygenase from *Pseudomonas cepacia* show a change of ligation state on substrate binding. *Biochemistry* **32**, 4820–4825.
29. Piepho, S.B. & Schatz, P.N. (1983). *Group Theory in Spectroscopy with Applications to Magnetic Circular Dichroism.* John Wiley & Sons, New York.
30. Fee, J.A., *et al.*, & Münck, E. (1984). Purification and characterization of the Rieske iron–sulfur protein from *Thermus thermophilus*. Evidence for a [2Fe–2S] cluster having non-cysteine ligands. *J. Biol. Chem.* **259**, 124–133.
31. Degli Esposti, M., Crimi, M., Samworth, C.M., Solaini, G. & Lenaz, G. (1987). Resolution of the circular dichroism spectra of the mitochondrial cytochrome bc_1 complex. *Biochim. Biophys. Acta* **892**, 245–252.
32. Degli Esposti, M., Ballester, F., Solaini, G. & Lenaz, G. (1987). The circular-dichroic properties of the 'Rieske' iron–sulphur protein in the mitochondrial ubiquinol:cytochrome *c* reductase. *Biochem. J.* **241**, 285–290.
33. Gebhard, M.S., Koch, S.A., Millar, M., Devlin, F.J., Stephens, P.J. & Solomon, E.I. (1991). Single-crystal spectroscopic studies of $Fe(SR)_4^{2-}$ (R = 2-(Ph)C_6H_4): electronic structure of the ferrous site in rubredoxin. *J. Am. Chem. Soc.* **113**, 1640-1649.
34. Gebhard, M.S., Deaton, J.C., Koch, S.A., Millar, M. & Solomon, E.I. (1990). Single-crystal spectral studies of $Fe(SR)_4^-$ [R = 2,3,5,6-$(Me)_4C_6H$]: the electronic structure of the ferric tetrathiolate active site. *J. Am. Chem. Soc.* **112**, 2217–2231.
35. Pavlosky, M.A. & Solomon, E.I. (1994). Near IR CD/MCD spectral elucidation of two forms of the non-heme active site in native ferrous soybean lipoxygenase-1: correlation to crystal structures and reactivity. *J. Am. Chem. Soc.*, in press.
36. Mabrouk, P.A., Orville, A.M., Lipscomb, J.D. & Solomon, E.I. (1991). Variable-temperature variable-field magnetic circular dichroism studies of the Fe(II) active site in metapyrocatechase: implications for the molecular mechanism of extradiol dioxygenases. *J. Am. Chem. Soc.* **113**, 4053–4061.
37. Twilfer, H., Bernhardt, F.H. & Gersonde, K. (1985). Dioxygen-activating iron center in putidamonooxin. Electron spin resonance investigation of the nitrosylated putidamonooxin. *Eur. J. Biochem.* **147**, 171–176.
38. Wende, P., Bernhardt, F.H. & Pfleger, K. (1989). Substrate-modulated reactions of putidamonooxin. The nature of the active oxygen species formed and its reaction mechanism. *Eur. J. Biochem.* **181**, 189–197.
38. Bill, E., Bernhardt, F.H., Trautwein, A.X. & Winkler, H. (1985). Mössbauer investigation of the cofactor iron of putidamonooxin. *Eur. J. Biochem.* **147**, 177–182.
40. Batie, C.J. & Ballou, D.P. (1990). Phthalate dioxygenase. *Methods. Enzymol.* **188**, 61–70.

Received: **20 Sep 1994**; revisions requested: **12 Oct 1994**; revisions received: **14 Oct 1994**. Accepted **17 Oct 1994**.